

In order to evaluate the experimental results objectively, physical stress in the experiment was evaluated with the mean value of musculoskeletal moment calculated based on the measured force as:

$$J_{\tau_m}(i) = \frac{1}{t_f} \int_0^{t_f} |\tau_m(t, i)| dt, \quad (12)$$

and the integral values of myoelectricity normalized with the maximum in the overall trials for estimating which muscle contributed to the experimental motion as:

$$J_{m_f}(i) = J_f(i) / J_{f_{\max}}, \quad (13)$$

$$J_{m_e}(i) = J_e(i) / J_{e_{\max}}, \quad (14)$$

where:

$$J_f(i) = \int_0^{t_f} |m_f(t, i)| dt, \quad (15)$$

$$J_e(i) = \int_0^{t_f} |m_e(t, i)| dt, \quad (16)$$

$$J_{f_{\max}} = \max\{J_f(1), \dots, J_f(n)\}, \quad (17)$$

$$J_{e_{\max}} = \max\{J_e(1), \dots, J_e(n)\}. \quad (18)$$

In (12)–(18), n and t_f represent number of trials for each operator and trial duration, respectively, $\tau_m(t, i)$ is the measured musculoskeletal moment, $J_{\tau_m}(i)$ is the mean value of the musculoskeletal moment, $m_f(t, i)$ and $m_e(t, i)$ are the myoelectricity values at the flexor and extensor muscle, respectively, and $J_{m_f}(i)$, $J_{m_e}(i)$ are the normalized myoelectricity values at the flexor and extensor muscle, respectively.

The Semantic Differential (SD) method was used for the evaluation of the operator's feeling as summarized in Table 3 [6, 9, 10] for the subjective evaluation of experimental results. In Table 3, operationality was defined as the feeling of whether an operator could swing the leg according to the his/her intention or not

Table 3.
Evaluation of the operator's feelings

	Mark						
	–3	–2	–1	0	1	2	3
Operationality	very bad	bad	slightly bad	—	slightly good	good	very good
Stress level	very heavy	heavy	slightly heavy	—	slightly light	light	very light

and the stress level as the feeling of 'light' or 'heavy'. As a reference for the feeling evaluated in the experiments, when the virtual impedance was not adjusted at all, the marks of the operability and stress level were set to 2 and -3, respectively. The operators were well rehearsed so as to understand the meaning of operability and stress level in the evaluation before the experiments. The experimental results were evaluated mainly with the musculoskeletal moment, which reflects the efficiency of motions.

4. RESULTS

4.1. Basic experiments for adjustment of virtual impedance

Figures 6–8 depict the experimental results of musculoskeletal moment and myoelectricity at the flexor and extensor muscles respectively. Panels (a)–(d) indicate the experimental data for adjustment of virtual inertia moment viscous friction, gravitational moment and Coulomb friction, respectively. The results were obtained from 220 trials for each operator, i.e., total of 660 trials.

The amount of musculoskeletal moment and myoelectricity tended to decline gradually with the decrease of the positive virtual inertia moment and virtual Coulomb friction in panels (a) and (b) of Figs 6–8.

In particular, the amount of musculoskeletal moment decreased markedly for operators A and B. In contrast, musculoskeletal moment and myoelectricity had a tendency to remain steady or increase slightly for the negative values of the virtual inertia moment and the virtual Coulomb friction, and it is likely that the negative virtual impedance made the experimental motion unstable.

In the case of the virtual gravitational moment in panel (c) of Figs 6–8, the amount of musculoskeletal moment tended to increase slightly. The changes of myoelectricity were divided depending on the operator into the case of rising slightly and the case of increasing and decreasing in turn. Hence, we could be fairly certain that the gravitational moment by exoskeleton of HAL-3 did not impede the operator's motion and it is possible that the operators could swing their lower thigh effectively by using the gravitational moment.

The results of experiments for the virtual viscous friction in panel (d) of Figs 6–8 were divided into the case of operator A, and the case of operators B and C. In the case of operator A, the amount of musculoskeletal moment and myoelectricity at the extensor muscle rose with the decrease of the virtual viscous friction, and myoelectricity at the flexor muscle changed irregularly compared to operators B and C. Thus, it is likely that operator A could not correspond properly to the change of virtual viscous friction although he tried to let the experimental motion stabilize by using the muscles. In the case of operators B and C, the decrease of virtual viscous friction made the musculoskeletal moment and the myoelectricity at the flexor increase gradually after it declined to a trough at the positive virtual viscous friction. The amounts of myoelectricity at the extensor muscles of operators A–C

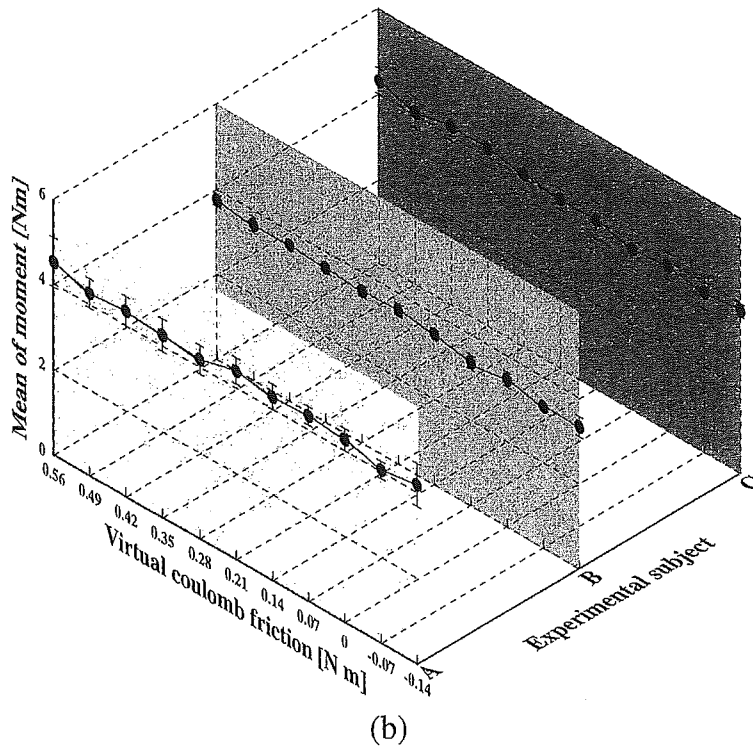
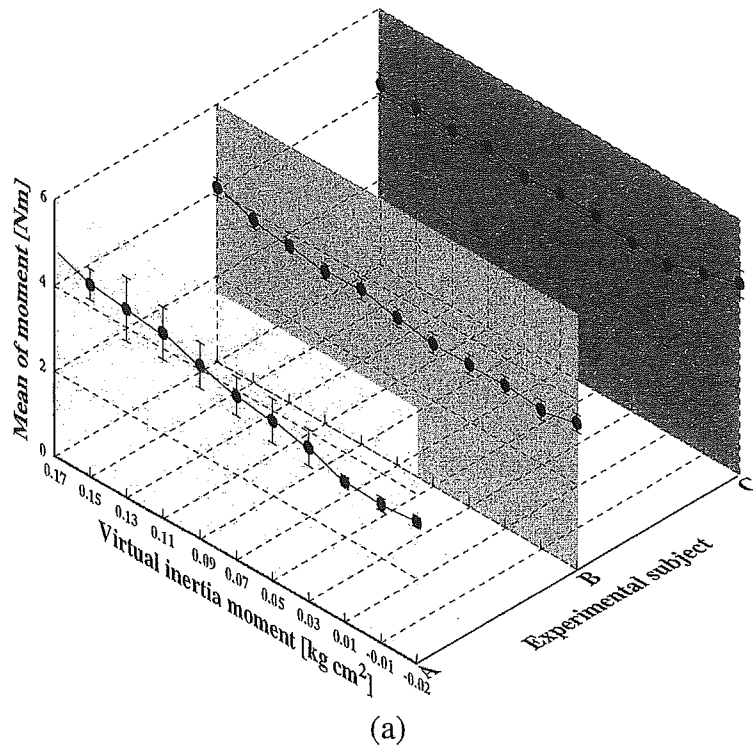
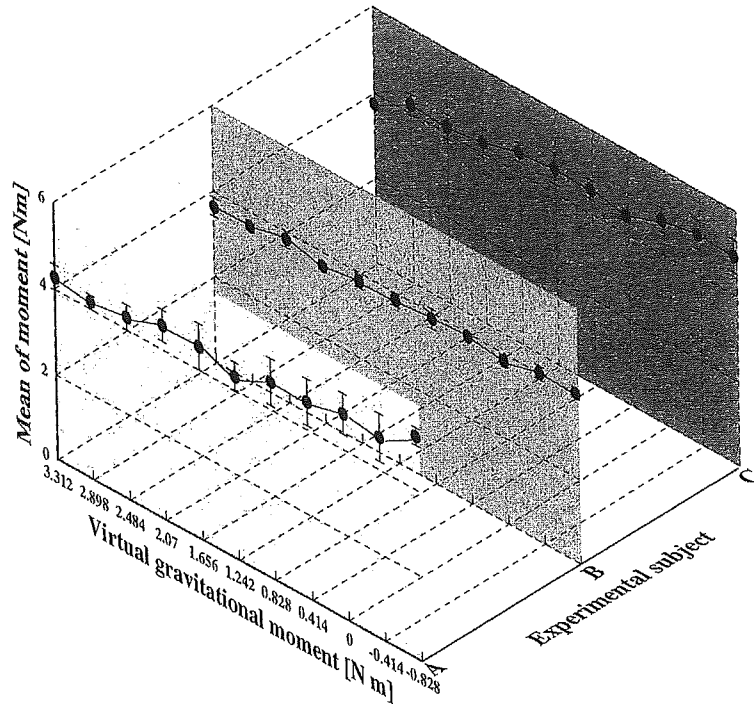
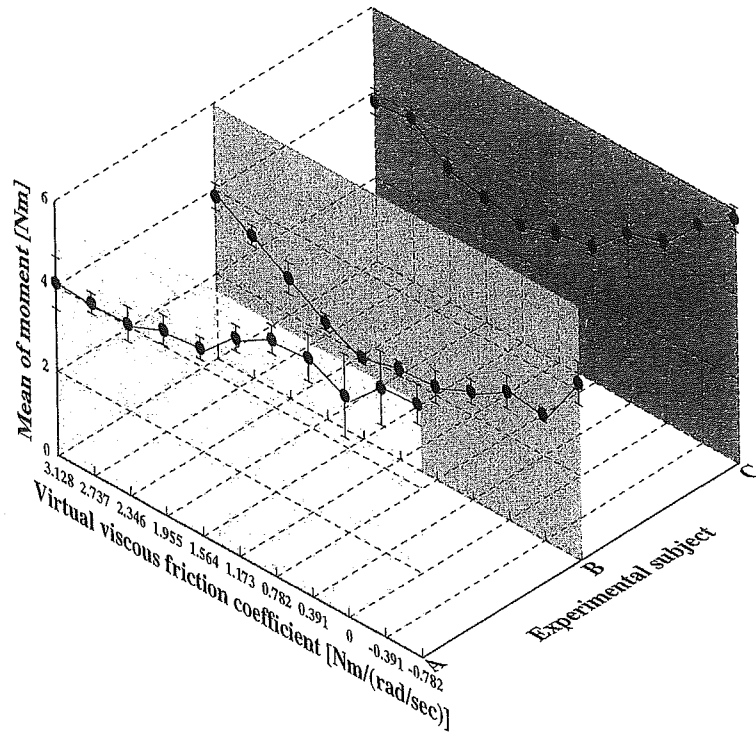


Figure 6. Experimental results for musculoskeletal moment.



(c)



(d)

Figure 6. (Continued).

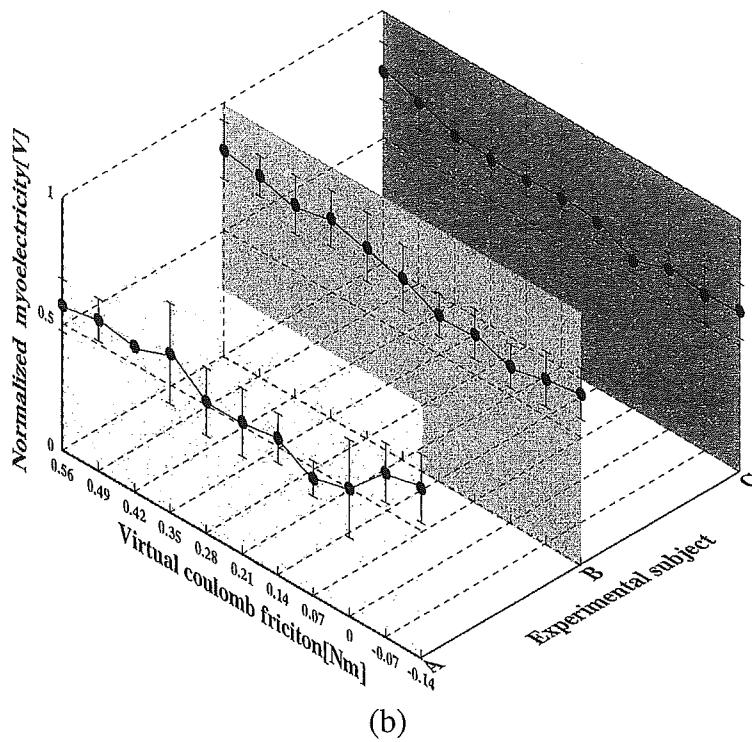
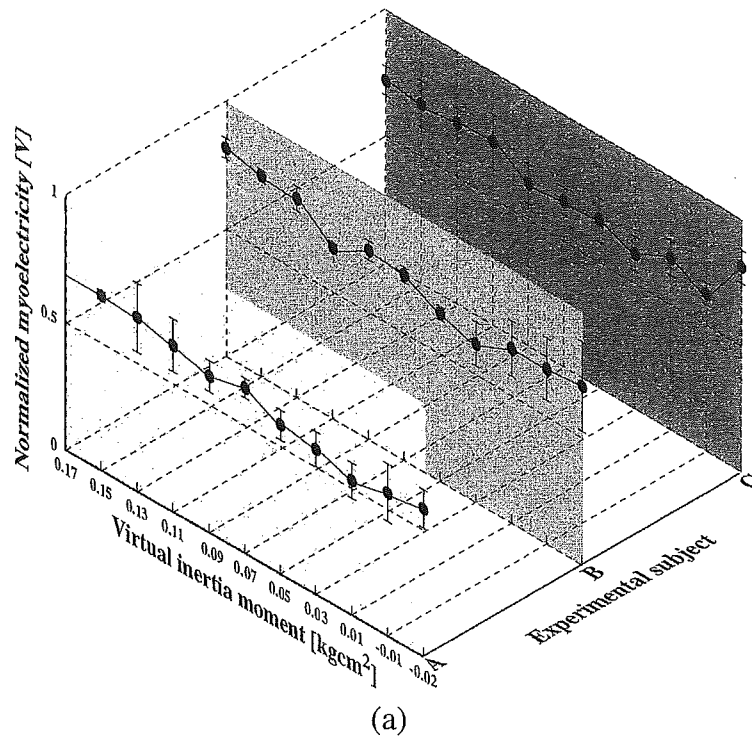


Figure 7. Experimental results for myoelectricity at the flexor muscle.

increased suddenly after they kept steady or increased slightly. Thus, what the results make clear is that the ideal virtual viscous friction for unconstrained motion was not zero. It is considered as the main cause of the results that the inertia

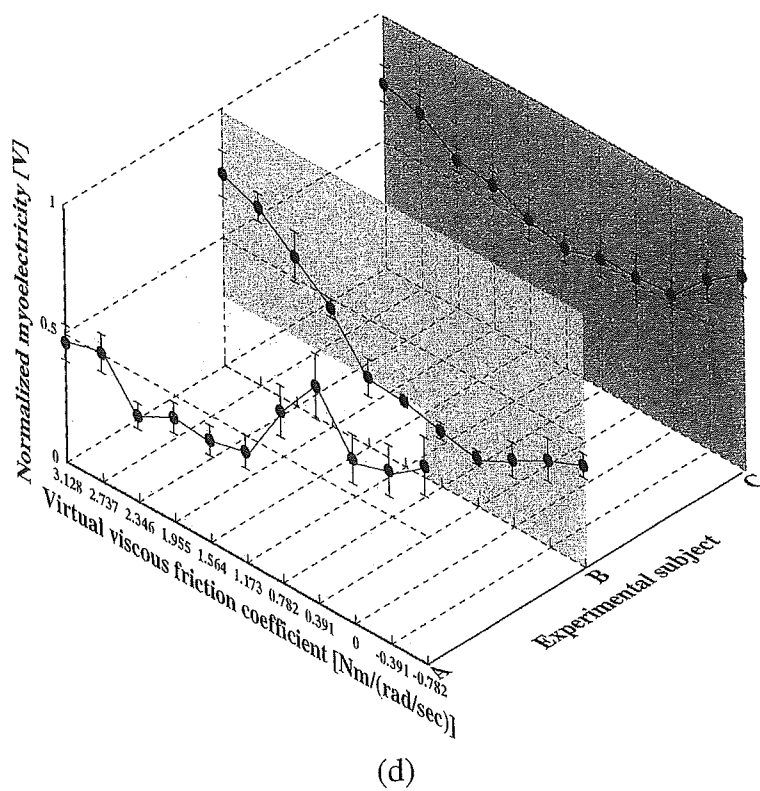
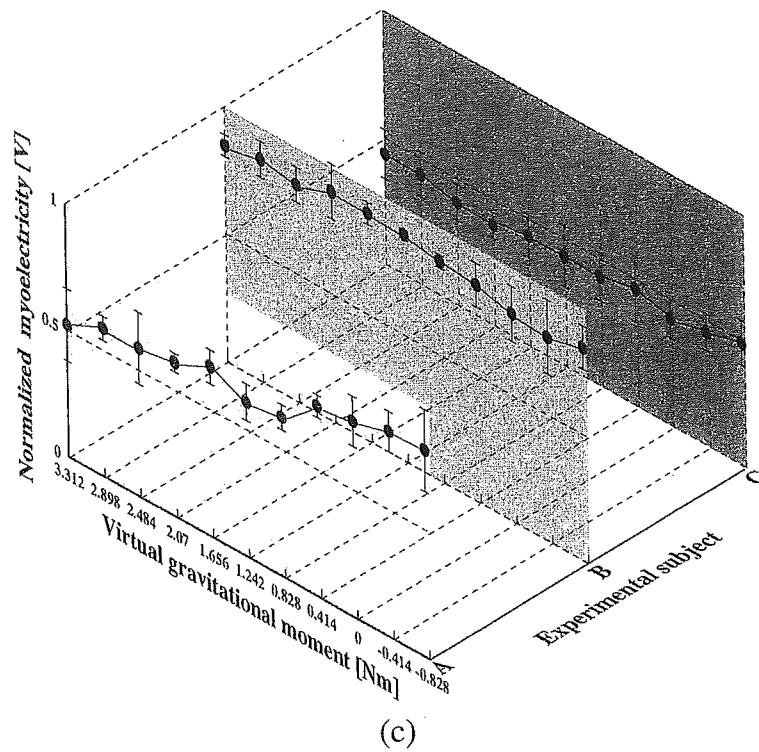


Figure 7. (Continued).

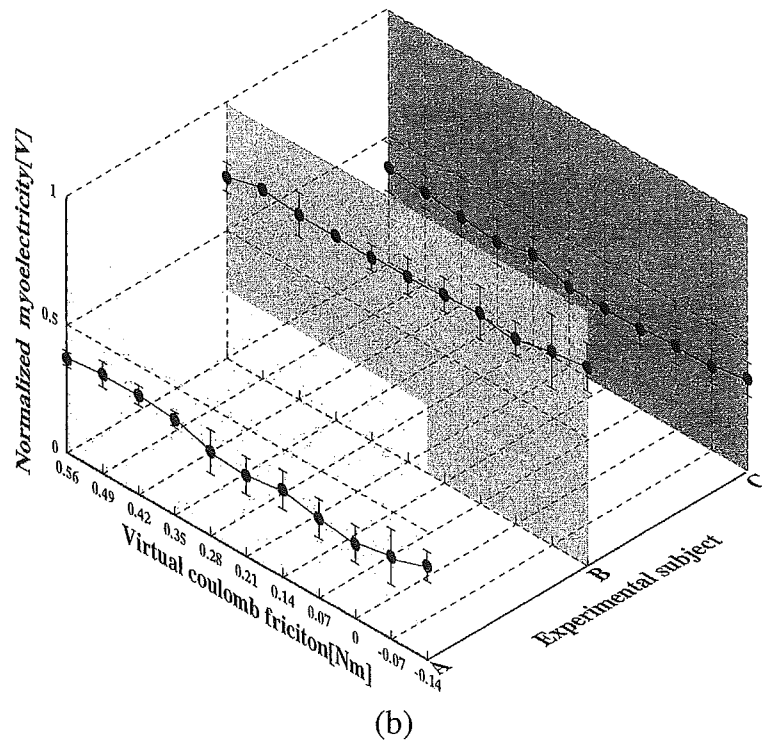
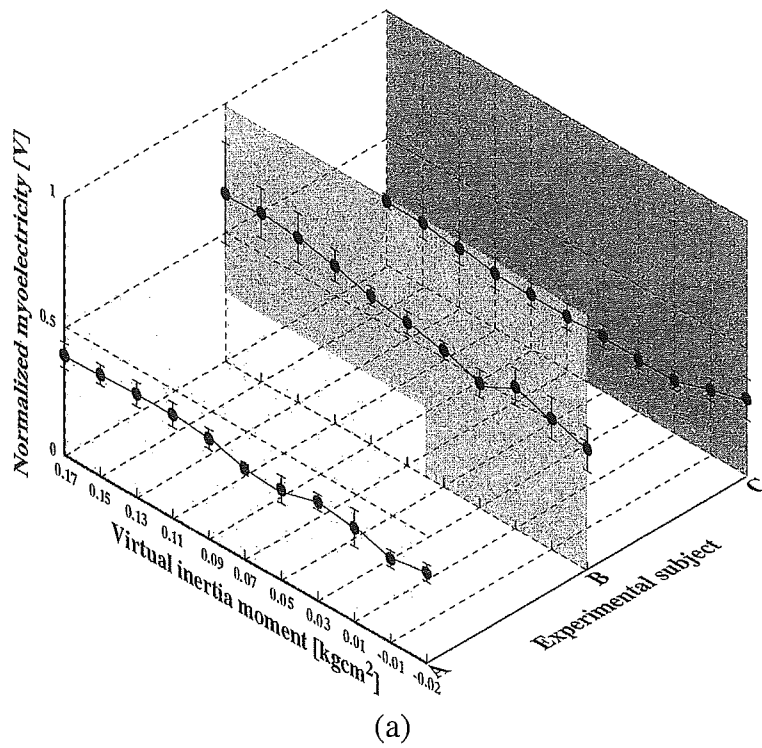


Figure 8. Experimental results for myoelectricity at the extensor muscle.

moment of the exoskeleton was large against the adjusted virtual viscous friction and the operators corresponded sensitively to the change of virtual viscous friction by increasing the impedance of muscles.

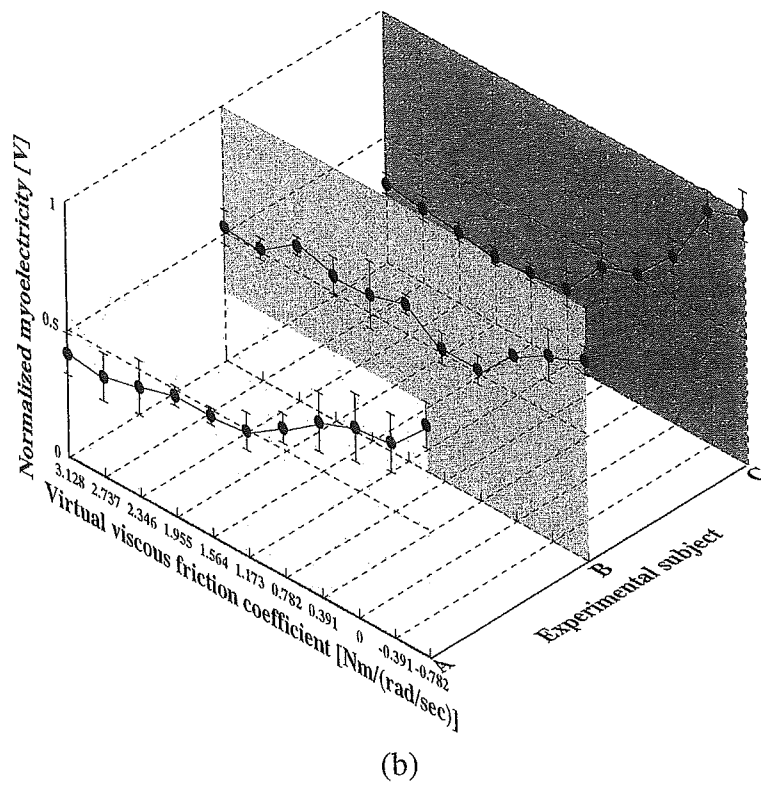
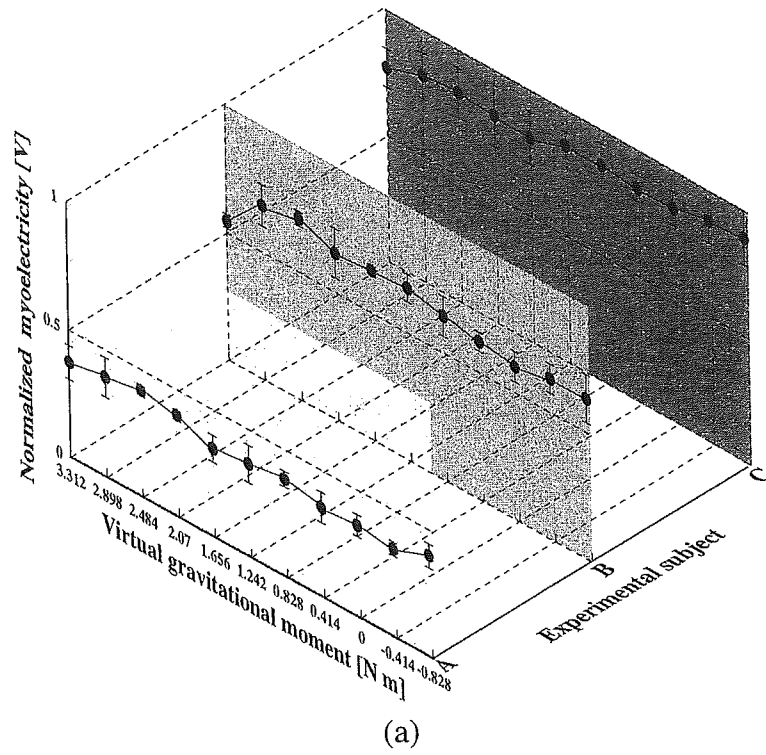


Figure 8. (Continued).

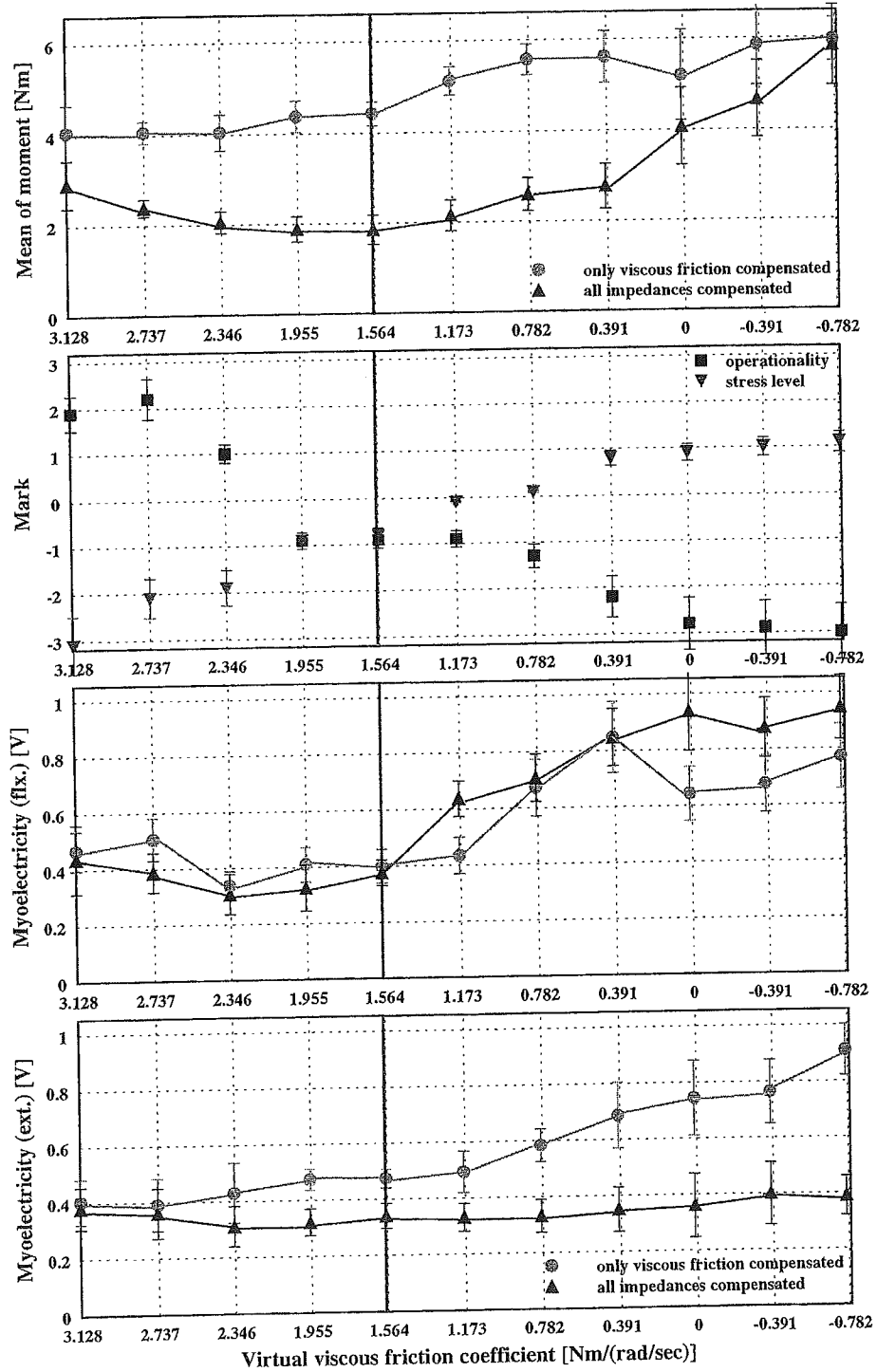
4.2. Experiments for adjustment of virtual impedance based on results of the basic experiments

Next, experiments for adjustment of the virtual inertia moment, viscous friction, gravitational moment and Coulomb friction were performed. Based on the results of the former experiments, the virtual inertia moment and the virtual Coulomb friction were set to zero. The virtual gravitational moment also needed to be adjusted properly to minimize the operator's physical stress, and its value was retained since the musculoskeletal moment and myoelectricity indicated the minimum values at the original gravitational moment of the exoskeleton. The virtual viscous friction was adjusted such as in the basic experiments and the experimental results were examined, again focused on the relationship between the change of the virtual viscous friction and the operators' physical stress. The experimental results were obtained from 220 trials for each operator.

Figure 9a–c shows the experimental data of the musculoskeletal moment, the operator's feelings and the myoelectricity at the flexor and extensor for operators A–C, respectively. The experimental results in panel (d) of Figs 6–8 are plotted as a graph of musculoskeletal moment and myoelectricity at the flexor and extensor with a shaded line, and vertical lines indicate the lowest points of the musculoskeletal moment with which the physical stress was mainly evaluated.

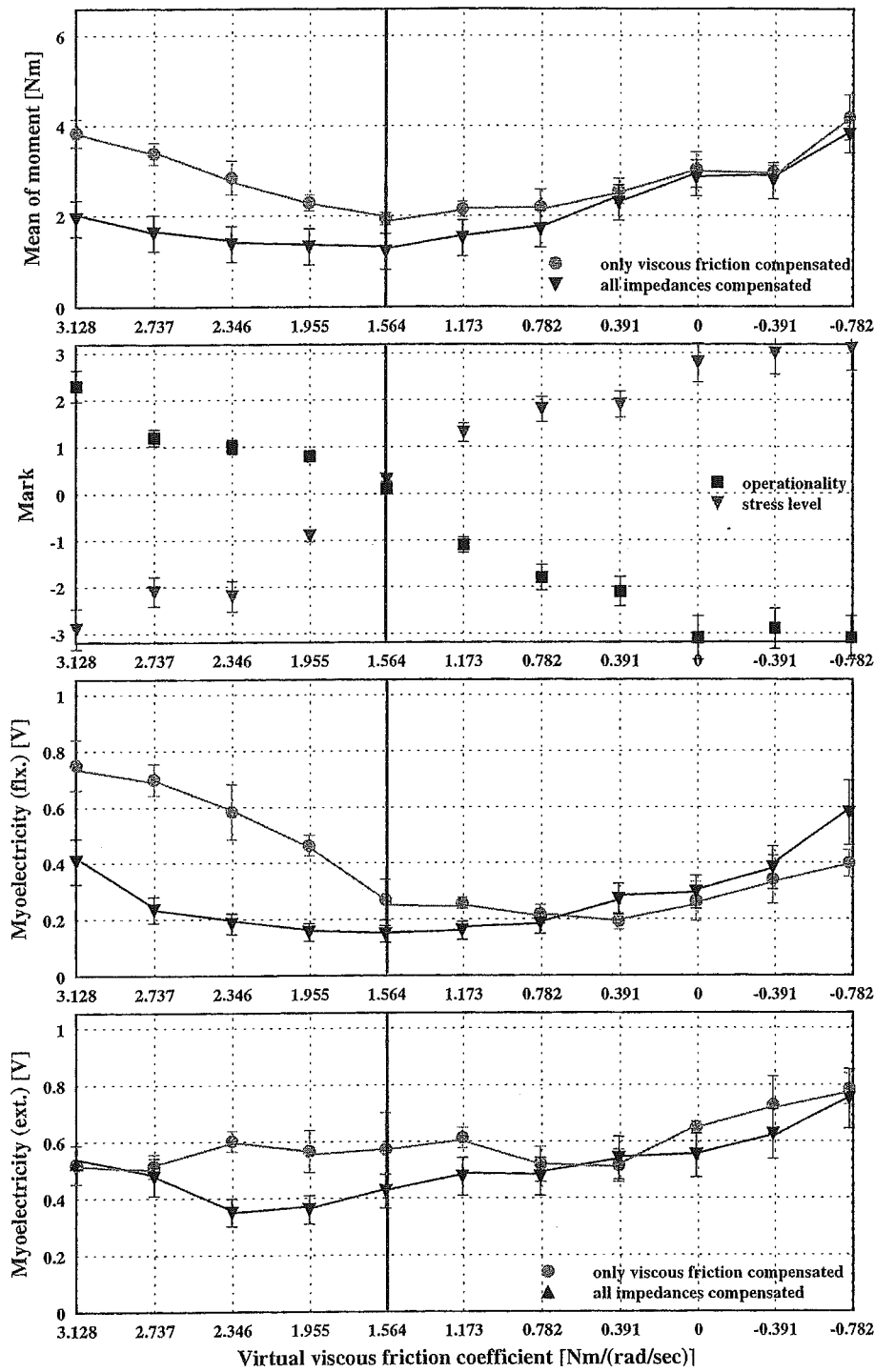
As an overall trend, the amounts of myoelectricity at the extensor and musculoskeletal moment decreased, and the myoelectricity at the flexor was reduced partially compared to the results in panel (d) of Figs 6–8. Hence, it is likely that the physical stresses by Coulomb friction and by inertia moment involving the decrease of the virtual viscous friction were reduced. However, the myoelectricity and musculoskeletal moment still increased at the lower value of virtual viscous friction, and, thus, it is likely that the operators increased the impedance of muscles against the reduced virtual viscous friction regardless of the adjustment of the virtual inertia moment.

The operability and stress level measured by the SD method became worse and lighter with the decrease of the virtual viscous friction. Focusing attention on the musculoskeletal moment, the data from operators A–C had the common feature that amounts were lowest, and the marks of operability and the stress level were in the range -1 to 1 , at $1.56 \text{ N m}/(\text{rad/s})$ of the viscous friction coefficient. Thus, the graphs of the musculoskeletal moment and the operators' feelings in Fig. 9 tell us that if the minimum musculoskeletal moment was prioritized in order to set the criteria for the effective unconstrained motion, the marks for both operability and stress level indicated medium values, and the virtual viscous friction was to be adjusted based on $1.56 \text{ N m}/(\text{rad/s})$. However, if the minimum myoelectricity was prioritized instead of the musculoskeletal moment, the virtual viscous friction coefficient should be higher than $1.56 \text{ N m}/(\text{rad/s})$, and the operability and stress level measured by the SD method became better and heavier, respectively. If the condition of the ideal virtual viscous friction to minimize the physical stress of



(a)

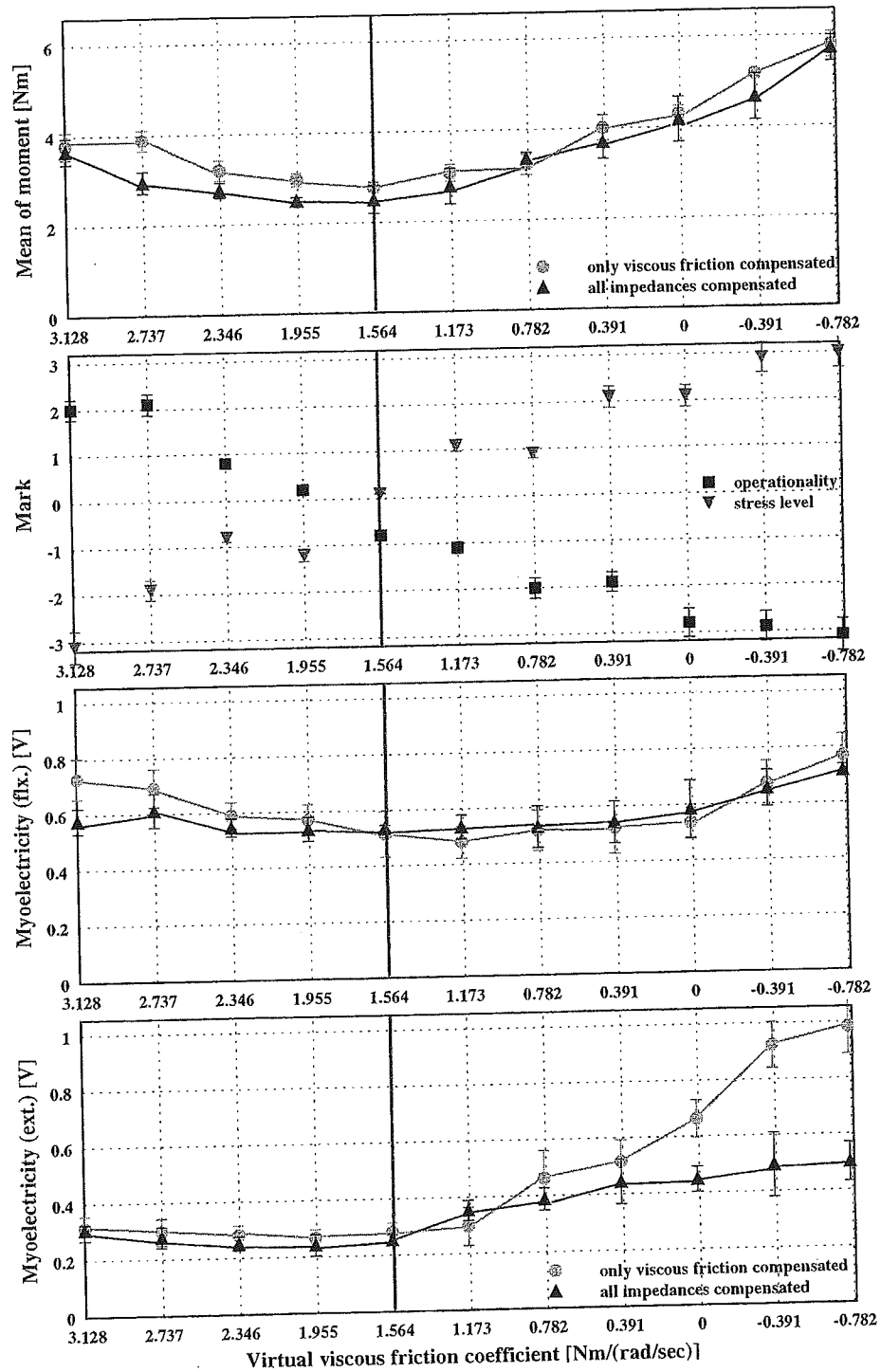
Figure 9. Experimental results for adjusting the virtual impedance based on the results of the basic experiments.



(b)

Figure 9. (Continued).

operators is to minimize the musculoskeletal moment and the muscle's activation as much as possible, the virtual viscous friction should be adjusted to a value a little higher than 1.56 Nm/(rad/s).



(c)

Figure 9. (Continued).

Therefore, based on the experimental results the criteria of the impedance adjustment for an exoskeletal robot assisting the unconstrained motion of the leg can be summarized as follows:

- (i) Set the virtual inertia moment and the virtual Coulomb friction to zero, respectively.
- (ii) The virtual gravitational moment should be retained.
- (iii) The virtual viscous friction should be adjusted to be a value a little higher than the value of the virtual viscous friction coefficient in order to minimize the musculoskeletal moment. In the case of HAL-3, the virtual viscous friction coefficient was adjusted based on a value a little higher than 1.56 N m/(rad/s).

5. DISCUSSION

In Fig. 9a–c, the myoelectricity, which represents the muscle activation, was a little higher than its minimum value at the virtual viscous friction which made the amount of musculoskeletal moment lowest. Thus, it is likely that human operators increased the impedance around the joint by antagonist muscle action to realize effective unconstrained motion of the leg.

The musculoskeletal moment of operator A in Fig. 6d became the lowest at the higher value of the virtual viscous friction and it is likely that operator A corresponded sensitively to the change of virtual viscous friction compared to operators B and C. The stress level of operator A in Fig. 9a became lower than that of operators B and C at the minimum value of the musculoskeletal moment. Differences in feelings to the same experimental motion or proficiency for experiments was considered as the main cause of the results.

The operability was not improved with the decrease of virtual viscous friction in the experimental result shown in Fig. 9 and it is considered that the viscous friction around HAL-3's actuators did not have any detrimental influence on the operability of the operator. If the myoelectricity that represents muscle activation is prioritized in the evaluation of physical stress, the operability has more influence on the human's feeling than the stress level in unconstrained motion.

The basic experiments for adjustment of the virtual inertia moment showed its influence on the operator's motion was comparatively small, although it was anticipated that the inertia moment of exoskeleton affected the musculoskeletal moment and muscle's activation greatly. The reason for this is that the inertia value was small compared that of a human [7] and the motions in the experiments were not rapid enough to be influenced by inertia change. However, it is expected that the influence of inertia moment will become larger when the change of angular velocity is very large.

6. CONCLUSIONS

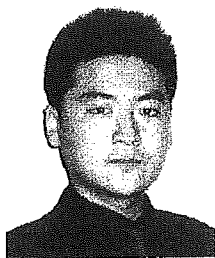
We examined and evaluated the relationships between the virtual impedance values and the physical stress of operators through experiments for unconstrained motions of the lower leg, and could establish the criteria for adjusting the virtual impedance

of the exoskeletal robot for the lower limb in order to minimize the operator's physical stress in unconstrained motion. It is likely that effective assist of the unconstrained lower limb, such as a swung leg in walking, can be realized by applying the established criteria in this paper to an exoskeletal robot for the lower limb.

REFERENCES

1. J. Okamura, H. Tanaka and Y. Sankai, EMG-based prototype powered assistive system for walking aid, in: *Proc. Asian Symp. on Industrial Automation and Robotics (ASIR '99)*, Bangkok, pp. 229–234 (1999).
2. T. Nakai, S. Lee, H. Kawamoto and Y. Sankai, Development of power assistive leg for walking aid using myoelectricity and linux, in: *Proc. Asian Symp. on Industrial Automation and Robotics*, Bangkok, pp. 1295–1310 (2001).
3. S. Lee and Y. Sankai, Power assist control for walking aid with HAL-3 based on EMG and impedance adjustment around knee joint, in: *Proc. IEEE/RSJ Int. Conf. on Intelligent Robots and Systems*, Lausanne, pp. 1499–1504 (2002).
4. H. Dankowicz, J. Adolfsson and A. B. Nordmark, Repetitive gait of passive bipedal mechanism in a three-dimensional environment, *J. Biomechan. Eng.* **123**, 40–46 (2001).
5. T. Tsuji, Y. Tanaka and M. Kaneko, Tracking control properties of human-robot systems, in: *Proc. 1st Int. Conf. on Information Technology in Mechatronics*, Istanbul, pp. 77–83 (2001).
6. Y. Yamada, H. Konosu, T. Morizono and Y. Umetani, Proposal of skill-assist: a system of assisting human workers by reflecting their skills in positioning tasks, in: *Proc. IEEE Int. Conf. on Systems, Man and Cybernetics*, Tokyo, pp. (IV)11–(IV)16 (1999).
7. S. Lee and Y. Sankai, Natural frequency-based power assist control for lower body with HAL-3, in: *Proc. IEEE Int. Conf. on Systems, Man, and Cybernetics*, Washington, DC, pp. 1642–1647 (2003).
8. E. Park and S. G. Meeek, Fatigue compensation of the electromyographic signal for prosthetic control and force estimation, *IEEE Trans. Biomed. Eng.* **40**, 1019–1023 (1993).
9. M. S. Ben-Lamine, S. Shibata, K. Tanaka and A. Shimizu, Impedance characteristics of robots considering human feelings, *JSME Int. J. (Ser. C)* **40**, 309–315 (1997).
10. H. I. Krebs, N. Hogan, M. L. Aisena and B. T. Volpe, Robot-aided neurorehabilitation, *IEEE Trans. Rehabilitation Eng.* **6**, 75–86 (1998).

ABOUT THE AUTHORS



Suwoong Lee received the BS degree in Electrical Engineering from Dong-A University, Korea in 1999, and the MS degree in Intelligent Interaction Technologies from the University of Tsukuba, Japan in 2002. He has been pursuing the PhD degree in the Doctoral Program in Intelligent Interaction Technologies, University of Tsukuba since 2002. His research interests include biomechanics, biorobotics and the human-machine interface including assistive exoskeletal robots and haptic devices. He is a member of the Robotics Society of Japan, and the Japan Society of Mechanical Engineers.



Yoshiyuki Sankai received the PhD degree in engineering from the University of Tsukuba, Japan in 1987. He was a JSPS research fellow, Assistant Professor, Associate Professor and Professor of Institute of Systems and Engineering in the University of Tsukuba, and a Visiting Professor of Baylor College of Medicine in USA. Currently, he is a professor and director of the prioritized research area 'New Robotics Frontier: Cybernics', Graduate School of System and Information Engineering in University of Tsukuba, Japan. His research interests include Robot Suit HAL (Hybrid Assistive Limb), the next generation artificial heart, humanoid Control, Bio-Medical Science, Network Medicine as related fields of Cybernics. He received a Grant of the Japanese Society for Artificial Organs (JSAO), Awards from American Society for Artificial Organs, International Society for Artificial Organs, International Society for Rotary Blood Pump with his students and so on. He was/is a president of Japan Society of Embolus Detection and Treatment, a chair of *International Journal of the Robotics Society of Japan*, a member of Awards Committee in the Robotics Society of Japan and Japan Society of Mechanical Engineers, an executive editor of Vascular Lab., an executive board member of Robotics Society of Japan, a founder and a chairman of CYBERDYNE Inc.

Control Method of Robot Suit HAL working as Operator's Muscle using Biological and Dynamical Information

Tomohiro Hayashi, Hiroaki Kawamoto and Yoshiyuki Sankai

Graduate School of Systems and Information Engineering
University of Tsukuba

1-1-1 Tennodai, Tsukuba-shi Ibaraki-ken, Japan

iros@golem.kz.tsukuba.ac.jp

Abstract - For assisting human motion, assistive devices working as muscles would be useful. A robot suit HAL (Hybrid Assistive Limb) has been developed as an assistive device for lower limbs. Human can appropriately produce muscle contraction torque and control joint viscoelasticity by muscle effort such as co-contraction. Thus, to implement functions equivalent to human muscles using HAL, it is necessary to control viscoelasticity of HAL as well as to produce torque in accordance with operator's intention. Therefore the purpose of this study is to propose a control method of HAL using Biological and Motion Information. In this method, HAL produces torque corresponding to muscle contraction torque by referring to the myoelectricity that is biological information to control operator's muscles. In addition, the viscoelasticities of HAL are adjusted in proportion to operator's viscoelasticity that is estimated from motion information by using an on-line parameter identification method. To evaluate the effectiveness of the proposed method, the method was applied to a swinging motion of a lower leg. When this method was applied, HAL could work like operator's muscles in the swinging motion, and as a consequence, the muscle activities of the operator were reduced. As a result of this experiment, we confirmed the effectiveness of the proposed method.

Index Terms - robot suit, viscoelastic properties, impedance control, on-line parameter identification, myoelectricity.

I. INTRODUCTION

Assistive devices that can work as motor organs would be useful for assisting or enhancing human motion. We have developed a robot suit HAL (Hybrid Assistive Limb) as an assistive device for operator's lower limb [1-3].

In order to use HAL as operator's muscles, HAL has to work as a torque generator like muscles. It is necessary that HAL detect operator's intention to produce muscle torque voluntarily, in order to produce torque. It is useful to use biological information such as myoelectricity to detect operator's intention [2, 4]. Additionally, the operator cannot only produce the muscle torque, but also control joint viscoelasticity by muscle effort such as co-contraction of the flexor and extensor [5, 6]. The joint stiffness is adjusted for different motions. When the operator needs a high joint viscoelasticity, it is useful to increase a viscoelasticity of an actuator of HAL for assistance. Hence, it is also necessary to control viscoelasticity of HAL adaptively by referring to operator's joint viscoelasticity. It is necessary to estimate

operator's viscoelastic properties using motion information because it is difficult to measure them directly.

Therefore, the purpose of this study is to propose a control method of the robot suit using Biological and Motion Information to use the robot as operator's joint muscles.

In this paper, the proposed method is applied to HAL Mark three (HAL-3) [2, 3] in the case of swinging motion of the lower leg. Fig. 1 shows the configuration of HAL-3. It consists of exoskeleton frame with actuators for knee and hip joints in each leg. The angle of each joint is measured with a potentiometer attached to the joint. To prevent hyperextension or hyperflexion, every actuator is equipped with mechanical limiters.

II. CONTROL METHOD OF HAL BY REFERRING TO OPERATOR'S BIOLOGICAL AND MOTION INFORMATION

A. Actuator Control based on Biological Information

In this section, we describe a method to produce torque corresponding to muscle contraction torque by actuators of HAL using the myoelectricity.

To detect myoelectricity, two sensor units are attached on operator's skin near the flexor and the extensor driving the targeted joint as shown in Fig. 2. The sensor unit consists of two electrodes and an instrumentation amplifier. Two signals of myoelectricity from the flexor and extensor are filtered and amplified. The myoelectric activity $E(t)$, which is an amplitude envelope of myoelectricity, is defined as follows:

$$E(t) = \sqrt{\frac{1}{T} \int_{t-T}^t m^2(t) dt} \quad (1)$$

where m is the measured myoelectricity. This equation is applied to both the flexor and extensor of the targeted joint. The myoelectric activity is calculated online.

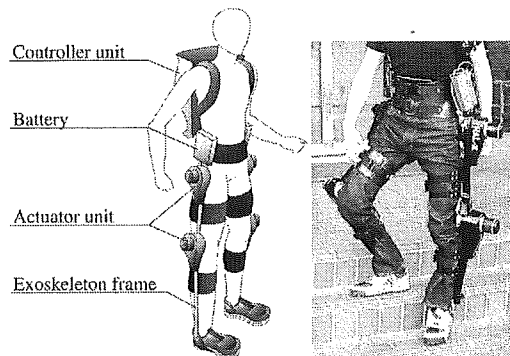


Fig. 1 Configuration of the robot suit HAL-3.

Then, the estimated muscle torque $\hat{\mu}$ is given by

$$\begin{aligned}\hat{\mu} &= \hat{\mu}_{ex} - \hat{\mu}_{flex} \\ &= (a_e E_e(t) + b_e) - (a_f E_f(t) + b_f)\end{aligned}\quad (2)$$

where $E_f(t)$ and $E_e(t)$ are the myoelectric activities of the flexor and extensor respectively, a_f , a_e , b_f and b_e are conversion coefficients from myoelectric activities to the contraction torque. By using estimated muscle torque, the torque τ_μ which HAL produces is given by

$$\tau_\mu = \alpha_\mu \hat{\mu}\quad (3)$$

where α_μ is a gain parameter.

A calibration exercise is necessary in order to obtain the conversion coefficients in (2). For the calibration, HAL has outputted steady torque pattern as a reference torque, and the operator putting on HAL has produced torque to compete against the reference torque without producing co-contraction as far as possible. The calibration exercise has been individually performed to the flexor and extensor of the joint. To obtain values of the conversion coefficients, a conventional least-square method has been applied. One of the results of the calibration exercise is shown in Fig. 3. The conversion coefficients apparently depend on operator's physical condition and the attached location of the sensor unit. Hence, the calibrating motion must be carried out, whenever the operator put on HAL.

B. Musculoskeletal Model of Operator's Lower Limb Working with HAL

We have constructed a musculoskeletal model of operator's lower limb equipped with the exoskeleton-actuator of HAL for estimating viscoelastic properties of operator's joint muscles and for controlling the properties of HAL.

In this study, muscles acting on a joint are regarded as one muscle group. Fig. 4 shows a model of muscle group around operator's knee joint as an example. The muscles in the group can respectively produce torque toward the contracting direction, but cannot produce it toward the extending direction. Thus, the muscle group needs two torque generators corresponding to the two directions.

Viscoelastic properties of the muscle group can be represented as a combination of a viscous element and an elastic element. We have assumed that the operator can modify the viscosity and elasticity with time. Hence, the two elements are defined as time-varying parameters.

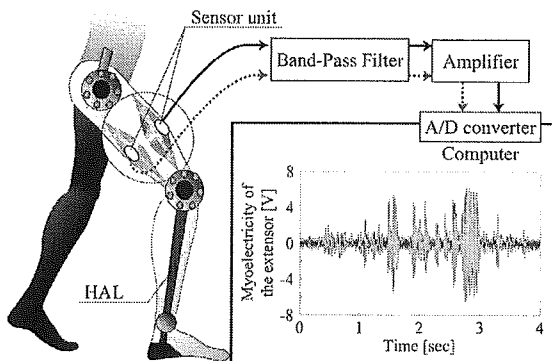


Fig. 2 Process of measuring myoelectricity.

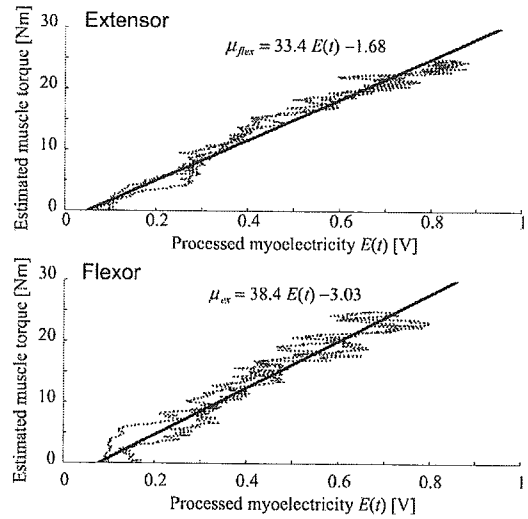


Fig. 3 One of the results of the calibration exercise.

Operator's leg with HAL is regarded as a multilink pendulum system to construct the musculoskeletal model. Fig. 5 shows the musculoskeletal model of operator's lower leg as an example. The motion equation of the i -th link of the model is expressed as follows:

$$I_i \ddot{\theta}_i + (D_i + R_i) \dot{\theta}_i + K_i \theta_i + M_i g l_i \sin \theta_i = \tau_i + \mu_i + \sigma_i\quad (4)$$

where θ is angle of a joint, I is total inertia around the joint, D and K are respectively the viscous and elastic coefficients of operator's muscle group, R is the viscous coefficients of the actuator of HAL, M is the mass of operator's leg link equipped with exoskeleton-actuator of HAL, g is the gravitational coefficient, l is the distance between the joint and the center of mass of operator's leg link with the exoskeleton, τ is torque produced by the actuator of HAL, μ is muscle torque produced by the operator, σ is the total interaction torque between adjacent links and suffix i is joint id. The parameters D and K are defined as time-depending parameters.

D. Method to Control Viscoelastic Properties of HAL

In this section we describe a method to control viscoelastic properties of HAL. In this study, actuator torque τ_ζ to control viscoelastic properties is determined based on impedance control method. τ_ζ of i -th joint is given by

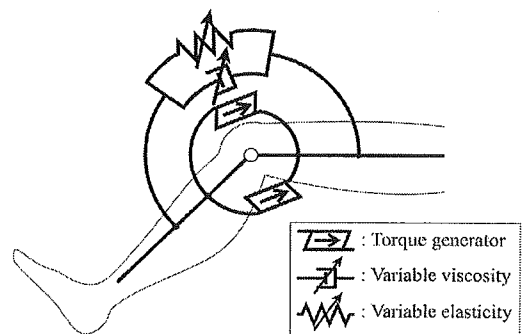


Fig. 4 Model of operator's muscle group around knee joint. Arrows in this figure mean contraction directions.

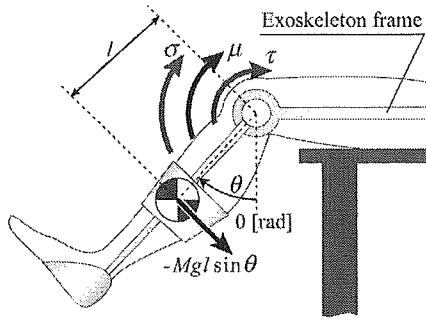


Fig. 5 Configuration of the musculoskeletal model of operator's lower leg equipped with HAL.

$$\tau_{i\zeta} = \alpha_{i\zeta} (-D_i \dot{\theta}_i - K_i \theta_i) \quad (5)$$

where $\alpha_{i\zeta}$ is a gain parameter.

In order that HAL works as muscles, the torque τ produced by its actuator is expressed as follows.

$$\tau_i = \tau_{i\zeta} + \tau_{i\mu} + \tau_{ic}. \quad (6)$$

where τ_{ic} is the torque to compensate mechanical impedance depending on exoskeleton-actuators of HAL [7, 8]. Although it is difficult to compensate all mechanical impedance of HAL absolutely, applying the compensation torque can sufficiently reduce the load derived from the impedance in actual use.

Substituting (6) into (4) gives

$$(I_i - I_{ih}) \ddot{\theta}_i + (1 + \alpha_{i\zeta}) D_i \dot{\theta}_i + (1 + \alpha_{i\zeta}) K_i \theta_i + M_i g l_i \sin \theta_i = (1 + \alpha_{i\mu}) \mu_i + \sigma_i. \quad (7)$$

This equation suggests that HAL produces actuator torque as if it amplified operator's muscle torque and viscoelastic properties according to the gain parameters $\alpha_{i\mu}$ and $\alpha_{i\zeta}$. In consequence, the proposed method would reduce loads on operator's muscles.

C. Estimation of Viscoelastic Properties of Operator's Muscle

In this section, we describe a method to estimate viscoelastic properties of operator's muscle group in real time in order to control viscoelastic properties of HAL. We take operator's lower leg as an example to describe the method to estimate operator's viscoelastic properties.

To linearize (4), some parameters are defined as

$$\begin{aligned} D' &= D + R \\ K' &= K + G(\theta) \\ G(\theta) &= \begin{cases} (Mgl \sin \theta) / \theta & (\theta \neq 0) \\ Mgl & (\theta = 0). \end{cases} \end{aligned} \quad (8)$$

By regarding the sum of τ , μ and σ as the input of the lower leg system, we can express the state-space form of the system (1) as follows.

$$\begin{cases} \frac{d}{dt} \begin{pmatrix} x_1(t) \\ x_2(t) \end{pmatrix} = \begin{pmatrix} 0 & 1 \\ -K'/I & -D'/I \end{pmatrix} \begin{pmatrix} x_1(t) \\ x_2(t) \end{pmatrix} + \begin{pmatrix} 0 \\ 1/I \end{pmatrix} u(t) \\ \theta(t) = (1 \ 0) \begin{pmatrix} x_1(t) \\ x_2(t) \end{pmatrix} \\ u(t) = \tau(t) + \mu(t) + \sigma(t). \end{cases} \quad (9)$$

We applied the Delta-Operator δ to the discrete-time form for realizing high sampling rate. For the state-space form

written as (9), the discrete-time form is given by

$$\begin{cases} \delta \begin{pmatrix} x_1(k) \\ x_2(k) \end{pmatrix} = \begin{pmatrix} 0 & 1 \\ -K'/I & -D'/I \end{pmatrix} \begin{pmatrix} x_1(k) \\ x_2(k) \end{pmatrix} + \begin{pmatrix} T_d/(2I) \\ (1-DT_d/(2I))/I \end{pmatrix} u(k) \\ \theta(k) = (1 \ 0) \begin{pmatrix} x_1(k) \\ x_2(k) \end{pmatrix}. \end{cases} \quad (10)$$

The solution of (10) for $\theta(k)$ gives

$$\begin{aligned} \theta(k) &= \varphi^T(k) \mathbf{X}(k) \\ \mathbf{X}(k) &= [e_1 - D'/I \ e_2 - K'/I \ T_d/(2I) \ 1/I] \\ \varphi(k) &= [\delta\theta(k)/E(\delta) \ \theta(k)/E(\delta) \ \delta u(k)/E(\delta) \ u(k)/E(\delta)] \end{aligned} \quad (11)$$

where $E(\delta)$ is a state variable. When $\hat{\mathbf{X}}(k)$ is defined as an estimated parameter vector, the prediction error $e(k)$ is given by

$$e(k) = \theta(k) - \hat{\theta}(k) = \theta(k) - \varphi(k) \hat{\mathbf{X}}(k). \quad (12)$$

By using weighted least-squares method, the update formula of the estimated parameter vector to minimize $e(k)$ is derived as follows.

$$\begin{aligned} \hat{\mathbf{X}}(k+1) &= \hat{\mathbf{X}}(k) + \mathbf{P}(k) \varphi(k+1) \frac{\theta(k+1) - \varphi^T(k+1) \hat{\mathbf{X}}(k)}{\rho + \varphi^T(k+1) \mathbf{P}(k) \varphi(k+1)} \\ \mathbf{P}(k+1) &= \frac{\mathbf{P}(k) - \mathbf{P}(k) \varphi(k+1) \varphi^T(k+1) \mathbf{P}(k)}{\rho + \varphi^T(k+1) \mathbf{P}(k) \varphi(k+1)} \\ \mathbf{P}(0) &= \beta \mathbf{I} \quad (\beta > 0) \end{aligned} \quad (13)$$

where ρ is a forgetting factor ($0 \ll \rho < 1$) and \mathbf{I} is the unit matrix of 4×4 .

To obtain parameters of the viscoelasticity of the muscle group, we should identify invariant parameters M , g , l and R in (4) before the estimation of the parameters of viscoelasticity. If the operator does not activate his muscles, the motion of operator's lower leg equipped with HAL can be expressed as follows.

$$I \ddot{\theta} + (D+R) \dot{\theta} + Mgl \sin \theta = \tau. \quad (14)$$

Additionally, the link model of the exoskeleton frame for the lower leg with the actuator of HAL is expressed as follows.

$$I_h \ddot{\theta} + R \dot{\theta} + M_h g l_h \sin \theta = \tau \quad (15)$$

where I_h is inertia around exoskeleton-actuator of HAL, M_h is the mass of the exoskeleton with the actuator, and l_h is the distance between the knee joint and the center of mass of the exoskeleton-actuator. Parameters in (14) and (15) have been beforehand identified [7-9].

To control the viscoelastic properties of HAL according to (5), it is necessary to know the angular velocity of the joint. In this study, the state observer is adopted. Applying a state observer to (10) gives

$$\begin{aligned} \delta \begin{pmatrix} x_1(k) \\ x_2(k) \end{pmatrix} &= \begin{pmatrix} 0 & 1 \\ -K'/I & -D'/I \end{pmatrix} \begin{pmatrix} x_1(k) \\ x_2(k) \end{pmatrix} + \begin{pmatrix} T_d/(2I) \\ (1-DT_d/(2I))/I \end{pmatrix} u(k) \\ &+ \begin{pmatrix} g_1(k) \\ g_2(k) \end{pmatrix} \{ \theta(k) - \hat{\theta}(k) \} \end{aligned} \quad (16)$$

where g_1 and g_2 are observer gains. These gains must be adjusted to keep stability of the state observer because the lower leg model shown in (4) is designed as a time-varying system. In addition, it is desirable that a time constant of the state observer remains smaller than the electromechanical delay [10] in order to ensure tracking performance of the

parameter estimation. We have, therefore, predefined the time constant of the state observer. Then, stable eigenvalues λ_1 and λ_2 for the observer have been defined for satisfying predefined time constant. Two observer gains have recursively been updated. The updating forms of observer gains are

$$\begin{aligned} g_1(k) &= \lambda_1 - \lambda_2 - D'(k)/I(k) \\ g_2(k) &= \lambda_1 \lambda_2 - g_1(k) D'(k)/I(k). \end{aligned} \quad (17)$$

III. EXPERIMENTS

To evaluating the proposed method, it was applied to a swinging motion of a lower leg. The operator putting on HAL sat on a chair that has enough height to prevent his foot from grounding. The operator swung his right lower leg up and down. The operator was asked not to actuate other joints except the right knee. We have assumed a combination of foot and lower leg as one link, because ankle joints have been locked. From the above conditions, σ in (4) can be ignored.

To evaluate effectiveness of the proposed method, two types of experiments were carried out. In the first experiment (Experiment 1,) no assisting method was applied. HAL produced only the torque τ_c in (6) compensating its mechanical impedance. In the second experiment (Experiment 2,) the proposed method was applied. Torque produced by the actuator of HAL in this experiment was calculated according to (6). The gain parameters α_μ and α_ζ in were defined as 1.0 and 0.5 respectively.

For the experiments, targeted frequency for the swinging motion was 0.5 Hz. Targeted maximum angles for the extending direction and the flexing direction were respectively 1.0 and -0.3 radians. However, the operator was not required to follow "exactly" the targeted angles. The operator could confirm angle of the joint by a computer display in real time. For the experiments, multiple rehearsals were carried out before each experiment. The operator rested sufficiently between trials to curb the influence of muscular fatigues on his motions and myoelectricity [11].

A strain of the exoskeleton frame was measured in order to evaluate force applied to operator's lower leg by HAL. The strain gauge was attached to the frame between the fastening equipment for the lower leg and the actuator of the knee joint as shown in Fig. 6. When operator's joint is fixed, the obtained signal is proportional to the actuator torque produced by HAL. In the swinging motion, the obtained signal is thought to include influences of dynamics of exoskeleton system of HAL. However, the influences of dynamics are thought to be enough smaller than the applied force by HAL. Therefore, in this paper, we assume that the obtained signal is proportional to the force applied to operator's leg by HAL. In all experiments, the strain gauge signal was not used at all for the control of HAL.

IV. RESULTS

A. Experiment 1 (Without Any Assisting Method)

Fig. 7 shows a typical cycle of the swinging motion without applying any assistance by HAL. Fig. 7-A shows transitions of the angle of the knee joint. Increase of the angle corresponds to the extension of the knee joint, and decrease of

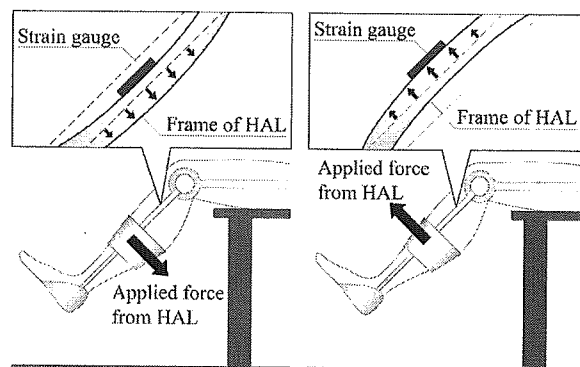


Fig. 6 Configuration to measure a strain of the exoskeleton-frame of HAL.

the angle corresponds to the flexion of the joint. To compare experimental results, we have defined swing-up phase and swing-down phase. The swing-up phase is defined as the period in which the angle and angular velocity of the knee joint are positive. The swing-down phase is defined as the period in which the angle and the angular velocity of the joint are positive and negative respectively.

Fig. 7-B shows myoelectric activities. The myoelectric activity of the extensor has been plotted as positive, and that of the flexor has been plotted as negative. Myoelectric activities of the extensor and flexor were approximately 0.1 [V] and 0.04 [V] respectively, whenever operator's muscles around the knee joint were relaxed in all evaluation experiments. During swing-up phase, the myoelectric activity of the knee extensor was predominant and the direction of the muscle torque was the same as the rotating direction of the knee joint. This result suggests that the extensor worked as an agonist. During swing-down phase, the myoelectric activity of the extensor was predominant, suggesting that operator's muscle torque was found in the opposite direction of the rotation of the knee joint. In addition, simultaneous activation of both the extensor and flexor has been observed in swing-down phases, which suggests a co-contraction of the extensor and flexor.

Fig. 7-C shows the strain of the exoskeleton frame. The strain signal has been defined as positive values, when torque derived from HAL acts on operator's lower leg in the extending direction. During swing-up phases, the strain signal was found negative. Thus, the force applied to the lower leg from HAL worked in the flexural direction. During swing-down phase, the strain signal remained almost positive, which suggests that the force acted in the extending direction. Therefore, HAL, which has not produced assisting torque, is thought to have approximately acted in the direction opposite to the rotation of the knee joint.

B. Experiment 2 (Using the Proposed Method)

Fig. 8 shows a typical cycle of the swinging motion in which the proposed method was applied. For a comparison, the cycle of swinging motion without any assisting method is superposed here as dotted lines. Fig. 8-A shows the transition of the angle of the actuator of the knee joint.

Myoelectric activities around the knee joint are shown in Fig. 8-B. In this experiment, the myoelectric activity of the

extensor was smaller than the activity in the case of not applying assisting method. In addition, the co-contraction of the extensor and flexor has hardly been observed.

The strain of the exoskeleton frame is shown in Fig. 8-C. In swing-up phases, the strain signal was approximately positive. In addition, in the middle of swing-down phase, the strain signal increased. These results signify the force applied to the lower leg from HAL worked in the extending direction.

C. Comparison of Experimental Results

To confirm the effectiveness of the proposed method, in this section, we compare results of two experiments by focusing on the swing-up phase and swing-down phase. Fig. 9-A and Fig. 9-B show the mean values of the average myoelectric activities per each phase. The average myoelectric activities decreased when the proposed method was applied. On the other hand, average myoelectric activities of the flexor in swing-up phases were approximately 0.04 [V]. These results signify that the operator has not used the flexor and any assisting method had no effect on the flexor in swing-up phases. The average myoelectric activities of the flexor in swing-down phases were approximately 0.8 [V] through all experiments. This result signifies that the proposed method had little effect on the flexor during swing-down phases.

Fig. 9-C and Fig. 9-D show the mean values of the average strain gauge signals per each phase. The average strain signal was negative in swing-up phases without any

assisting method. This result suggests that HAL acted on operator's knee joint in the flexing direction. In contrast, the average strain signals in swing-up phases were positive, when the proposed method was applied. These results suggest that HAL has effectively acted on operator's knee joint in the extending direction. Fig. 9-D suggests that HAL has most strongly acted on operator's knee joint in the extending direction during swing-down phases when the proposed method was applied.

V. DISCUSSION

The swinging motion of the knee joint was carried out to confirm the effectiveness of the proposed method. In swing-up phases through the experiments, the extensor worked as the agonist and simultaneously the flexor was relaxed. Therefore we consider that the role of operator's muscles in swing-up phases was to produce the voluntary contraction torque to extend his knee joint. On the other hand, in swing-down phases, myoelectric activities of extensor were predominant. In addition, co-contractions of the extensor and flexor were observed, when the proposed method was not applied. Therefore, we consider that the major role of operator's muscles in swing-down phases was to restrain the flexion of his knee joint appropriately.

In Experiment I, The strain gauge signal was not zero

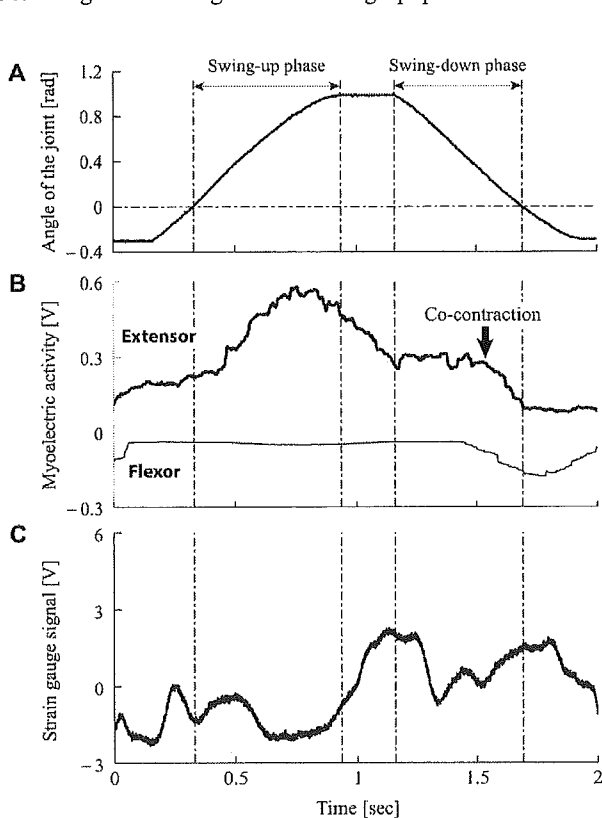


Fig. 7 A typical cycle of the swinging motion when no assisting method was applied

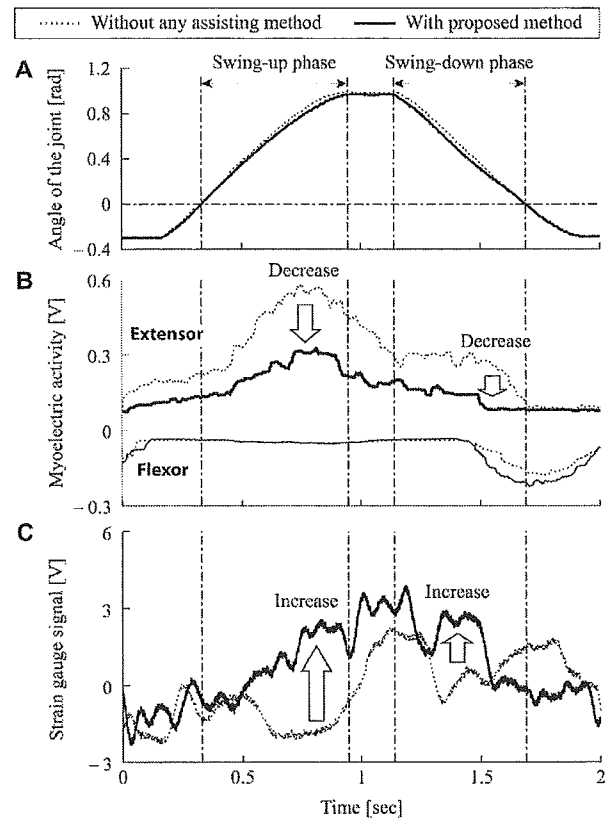


Fig. 8 A typical cycle of the swinging motion with applying the proposed method. Time-axis of this figure has been tuned so that the phase of the figure corresponds to those of Fig. 7.